Effect of Proton on Potassium Ion in Countertransport across Fine Porous Charged Membranes

Hidetoshi Matsumoto,[†] Akihiko Tanioka,*[,†] Tatsuji Murata,[†] Mitsuru Higa,[†] and Ken Horiuchi[‡]

Department of Organic and Polymeric Materials, Tokyo Institute of Technology 2-12-1 Ookayama Meguro-ku, Tokyo 152, Japan, and Material Analysis Research Center, Teijin Ltd., 4-3-2, Asahi-ga-oka, Hino-shi, Tokyo 191, Japan

Received: July 8, 1997; In Final Form: March 6, 1998

Proton and potassium ions countertransport across perfluorocarbon-type (Nafion) and hydrocarbon-type (K-101) cation-exchange membranes was studied, and the effect of proton transport on potassium ion transport was examined. It is considered that the fixed charge groups are distributed heterogeneously in the former and homogeneously in the latter. The experimental results were compared with calculated values using the Teorell−Meyer−Sievers's theory, which formulated transport phenomena based on the Donnan equilibrium and the Nernst−Planck flux equation. In the case of the K-101 membrane, the experimental results comparatively agreed with theoretical predictions. The deviation is attributed to the low estimation of the membrane effective charge density. On the other hand, the experimental results did not agree with theoretical predictions in the case of the Nafion membrane. It might be attributed not only to the low estimation of the membrane effective charge density but also to the high proton mobility caused by the charge transfer through structured water in the membrane pore.

1. Introduction

Proton transport has been attracting attention in biology, physiology, physical chemistry, and bioengineering. In a metabolic system, proton transport plays an important role; that is, H^+-ATPase converts a proton gradient into energy for ATP synthesis.[1] In amino acid transport through an ion-exchange membrane, protons facilitate or delay transport depending on the membrane surface condition, which is called interfacial transport.[2] The proton itself also has the largest ion mobility in aqueous solution, which is about 10 times that of Li^+,[3] and a peculiar transport mechanism called the *proton jump*.[4]

The structure of a biological membrane is tremendously complex and heterogeneous.[5] Moreover, there are multicomponent ion transport systems combined with the fields of chemical reaction in vivo. Consequently, it is very difficult to describe theoretically the transport phenomena of protons across biomembranes even at this moment. Also in the case of an artificial membrane, ionomer membranes whose fixed charge groups are distributed inhomogeneously and form a complex structure such as ion clusters have appeared recently. Nafion, composed of perfluorosulfonated carbon, is one of the typical ionomer membranes, which are applied for use in chlor-alkali cells,[6] fuel cells,[7] batteries,[8,9] water electrolyzers,[10] and gas separation.[11,12] Transport of water, ions, and gases within the ionometric material is intimately related to the polymer microstructure. Especially the proton has extremely high permeability. Gierke et al. suggested that ion clusters of approximately 5-nm diameter were connected by 1-nm diameter channels on the basis of X-ray and hydraulic permeability data.[13] Nafion also shows superselectivity where the Donnan equilibrium[14,15] cannot exert much influence. Reiss et al. indicated that this might be due to the inhomogeneity which possibly resulted from dipole clustering of fixed ionic groups.[16] Recently, many studies have been carried out in order to understand the role of water in proton transport using dielectric relaxation, conductivity, or NMR measurements.[17−21]

In this study, we used two kinds of typical artificial charged membranes, which were the perfluorocarbon-type and the hydrocarbon-type, to observe the transport phenomena of each ion in a three-component system composed of proton, potassium ion, and chloride ion as a common co-ion because multiionic systems are important to both synthetic and biological membranes. The fixed charge groups are considered to be distributed heterogeneously in the former and homogeneously in the latter. In addition, the experimental results were compared with calculated values using the Teorell−Meyer−Sievers theory (TMS theory),[22−24] which formulated transport phenomena based on the Donnan equilibrium and the Nernst−Planck flux equation, if the fixed charge groups were assumed to be distributed homogeneously in the ideal charged membranes. Finally, the effect of proton transport on the transport of other ions was examined by comparison with perfluorocarbon-type and hydrocarbon-type membranes.

2. Theoretical Background

The theoretical background of analysis is explained briefly in the following section.

2.1. Donann Equilibrium. The Donnan equilibrium for the *i*th species ion between a membrane and an external solution can be realized as[25]

$$\frac{\overline{C_i}}{C_i} = \exp\left(-\frac{Fz_i\Delta\phi_{\mathrm{don},j}}{RT}\right) = K_j^{z_i} \qquad (1)$$

* To whom correspondence should be addressed.
† Tokyo Institute of Technology.
‡ Teijin Ltd.

S1089-5647(97)02223-2 CCC: $15.00
Published on Web 05/30/1998

where $\overline{C_i}$ and C_i are the ith species ion concentration in the membrane and solution, respectively. $K_j^{z_i}$ and $\Delta\phi_{\mathrm{don},j}$ are the Donnan equilibrium constant and the Donnan potential at side j of the membrane surface, respectively. F, R, T, and z_i are Faraday's constant, the gas constant, the absolute temperature, and the valence of the ith species ion, respectively. An electroneutrality condition in the membrane requires

$$\sum z_i \overline{C_i} + z_x C_x = 0 \tag{2}$$

where z_x is the valence of the fixed charge group and C_x is the fixed charge density of the membrane. Equation 3 is obtained by substituting eq 1 into eq 2:

$$\sum z_i K_j^{z_i} C_i + z_x C_x = 0 \tag{3}$$

K is obtained only from the concentration of the outer solution C_i and the membrane fixed charge density C_x using eq 3; therefore, the concentration of the *ith* species ion in a membrane C_i is obtained from K and C_i using eq 1.

2.2. Calculation of *i*th Species Ion Flux. In an experimental system, a charged membrane is placed between two cells (side I and side II), and the cells are filled with electrolyte solutions. Thus, each ion flux can be obtained analytically under the assumption of a constant electric field or a constant ion concentration gradient in a charged membrane. For a constant ion concentration gradient, each ion flux is given by the following equation[26]

$$J_i = -\omega_i RT \frac{\overline{C_i^{\mathrm{II}}} - \overline{C_i^{\mathrm{I}}}}{d} - z_i F \omega_i \left(C_{i+} \frac{\overline{C_i^{\mathrm{II}}} - \overline{C_i^{\mathrm{I}}}}{d} x \right) \frac{\mathrm{d}\bar{\phi}}{\mathrm{d}x} \tag{4}$$

where d and ω_i are the membrane thickness and the ith species ion's mobility, respectively. The total electric current in a membrane equals zero

$$\sum_i z_i F J_i S = 0 \tag{5}$$

where S is the sectional area of a membrane. Equation 6 is obtained by integrating eq 4 and substituting it into eq 5

$$\Delta\bar{\phi} = -\frac{RT}{F} \frac{\sum_i z_i \omega_i (\overline{C_i^{\mathrm{II}}} - \overline{C_i^{\mathrm{I}}})}{\sum_i z_i^2 \omega_i (\overline{C_i^{\mathrm{II}}} - \overline{C_i^{\mathrm{I}}})} \ln \frac{\sum_i z_i^2 \omega_i \overline{C_i^{\mathrm{II}}}}{\sum_i z_i^2 \omega_i \overline{C_i^{\mathrm{I}}}} \tag{6}$$

Equation 7 is obtained from eq 4 by integrating across the membrane, from $x = 0$ to $x = d$:

$$J_i = -\frac{R\Delta\bar{\phi}}{d} \frac{z_i \omega_i (\overline{C_i^{\mathrm{II}}} - \overline{C_i^{\mathrm{I}}})}{\ln\left(\dfrac{\overline{C_i^{\mathrm{II}}}}{\overline{C_i^{\mathrm{I}}}}\right)} - \frac{RT}{d} \omega_i (\overline{C_i^{\mathrm{II}}} - \overline{C_i^{\mathrm{I}}}) \tag{7}$$

We can simulate the permeability of each ion across a charged membrane by expressing the time evolution of each ion concentration on both sides of a membrane using the flux solved by eq 7.

3. Experimental Section

3.1. Materials. A hydrocarbon-type cation exchange membrane shown in Figure 1a (K-101, Asahi Chemical), whose fixed charge groups were distributed homogeneously, and a perfluorocarbon-type cation exchange membrane shown in Figure 1b (Nafion N-117, Du Pont), whose fixed charged groups were distributed inhomogeneously, were used. Their physicochemical properties are shown in Table 1. Prior to use, Nafion was boiled in distilled water for 30 min for conditioning. Both membranes were then converted to the K^+ from the H^+ form by soaking in stirred 2M KCl for over 24 h, followed by washing with deionized water sufficiently.

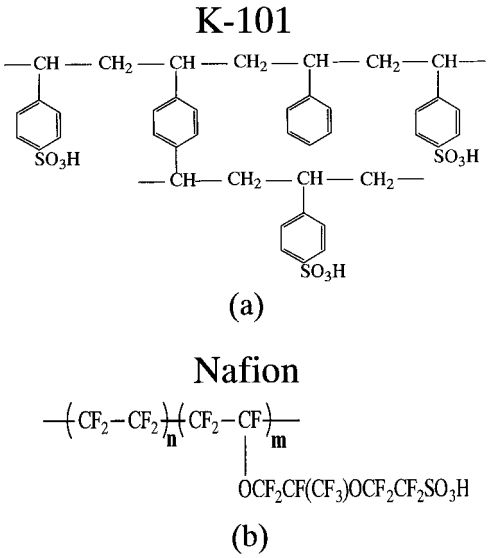

Figure 1. Chemical structure of (a) K-101 and (b) Nafion.

TABLE 1: Physicochemical Properties of Charged Membrane

	K-101	Nafion
effective charge density (mol/L)	0.68	0.29
charge density (mol/L)	5.53	3.12
water content (wt %)	24.4	29.6
degree of hydration	0.20	0.34
thickness (mm)	0.22	0.21
conductivity (mS/cm)		
0.5 mol/L KCl	93.9	36.4
0.5 mol/L HCl	94.3	196.9

HCl and KCl (Wako Pure Chemical Industries, Ltd.) were used as electrolytes.

3.2. Measurements of Time Dependence of Membrane Potential. First, we measured the time dependence of the membrane potential to determine the steady states in these charged membranes and three-component ion systems. A charged membrane was installed in the measuring cell as shown in Figure 2. The cell was made of acrylic resin composed of two compartments, and the area of the membrane exposed to solution was 3.14 cm^2. Three hundred milliliters of 0.05 M KCl was poured into the left compartment of the measuring cell, and the same content of 0.05 M HCl was poured into the right one. A schematic diagram of the experimental conditions in the initial state is shown in Figure 3. Measurements were made using an ion meter (IM-40S, TOA) and an Ag−AgCl electrode (HS-205C, TOA). A salt bridge was placed between the compartment of the cell and the electrode when each measurement was performed. All measurements were carried out in a stirred solution thermostated at 25.0 ± 0.1 °C under N_2 atmosphere.

3.3. Determination of Ion Concentrations. We set up an experiment on ion transport using the same experimental conditions and the same cell as mentioned above. Two milliliter sample solutions were collected using an autopipet from both

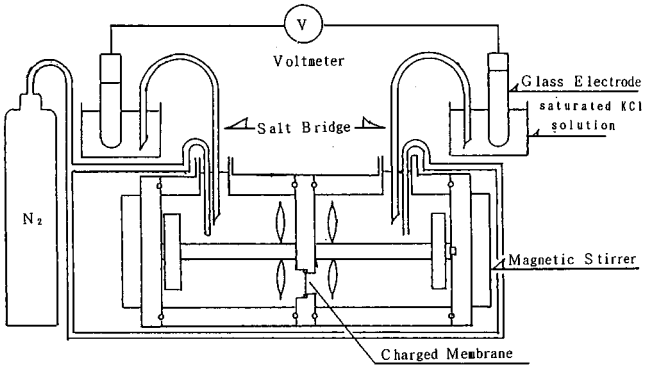

Figure 2. Apparatus for membrane potential and ionic transport measurements.

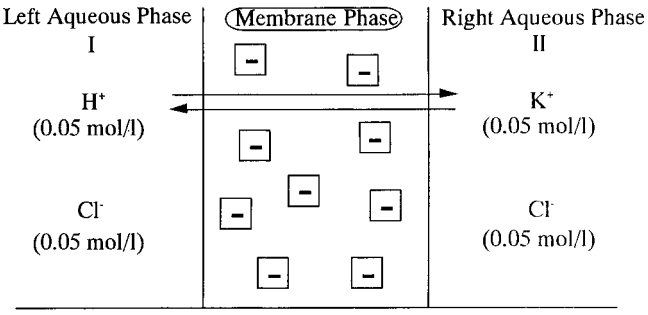

Figure 3. Schematic diagram of experimental conditions in initial state.

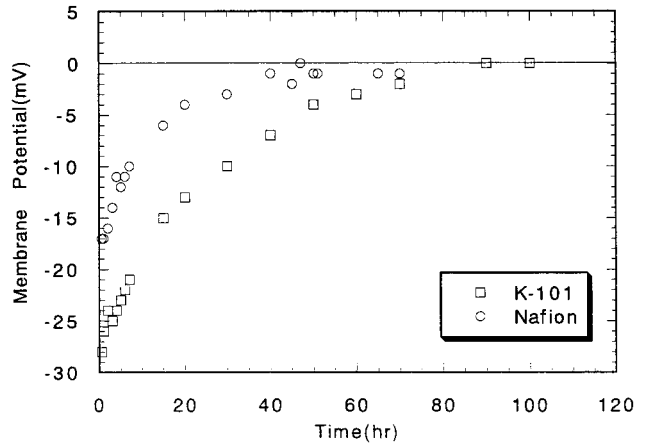

Figure 4. Variation of membrane potential as a function of time.

sides of the cell at every sampling. After a 0.5 mL sample solution was diluted to 100 mL, the concentration of H^+ was determined by potentiometric titration, and the concentrations of K^+ and Cl^- were determined by ion chromatography. The former was performed with 0.01N KOH as titrant using a pH meter (HM-60,TOA) and a pH combination glass electrode (GST-511C, TOA) in the stirred solution thermostated at 25.0 ± 0.1 °C under N_2 atmosphere. The latter was done using a column (#2720, used for cation analysis, and #2710, used for anion analysis), a conductivity detector (L-3720), an intelligent pump (L-6200), a column oven (655A-52, used at 40 °C), and a Chromato-Integrator (D-2500), which were made by Hitachi, Ltd.

4. Results and Discussion

4.1. Experimental Results. The time evolution of membrane potential is shown in Figure 4. The solid and broken lines represent K-101 and Nafion, respectively. The decrease

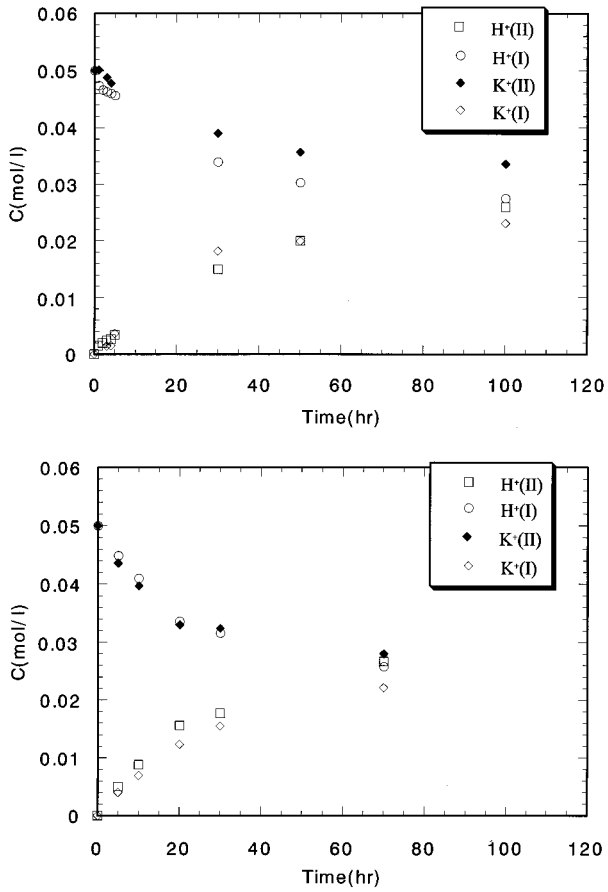

Figure 5. Changes in cation concentration on both sides (I and II) of the membranes as a function of time: (a, top) K-101 and (b, bottom) Nafion.

in membrane potential indicates that H^+ and K^+ are mixed in both sides. If both cations are mixed completely, the membrane potential becomes zero. These data tell us that both cations in Nafion are easily mixed compared with those in K-101. The changes in cation and anion concentrations on both sides of the membranes (I and II) as a function of time are shown in Figures 5 and 6, respectively. The cation concentration for K-101 is given as a function of time in Figure 5a and for Nafion in Figure 5b. Square and circle represent the concentration change of H^+, and black and white rhombuses that of K^+ in side II and side I, respectively. Similarly, the anion concentrations for K-101 are given as a function of time in Figure 6a and for Nafion in Figure 6b. Square and circle represent the concentration change of Cl^- in side II and side I, respectively. Considering the cations, H^+, which had the largest ion mobility in cations, was transported faster than K^+ for both K-101 and Nafion. One could recognize that the gap in the K^+ concentration between sides I and II closed and there was no difference in the H^+ concentration between sides I and II, if the membrane potential attained zero. On the other hand, with regard to anions, the difference in Cl^- concentration between sides I and II increased with time. This suggests that a small quantity of Cl^- moves together with the same content of H^+ in this counter-transport system, because electroneutrality applies throughout this system and the mobility of H^+ is much greater than that of K^+.[3] This is the evidence that the mobility in Nafion was faster than that in K-101 in this system.

The physicochemical properties of the charged membranes used here were characterized in advance and listed in Table 1. The effective charge density QC_x was given by fitting the

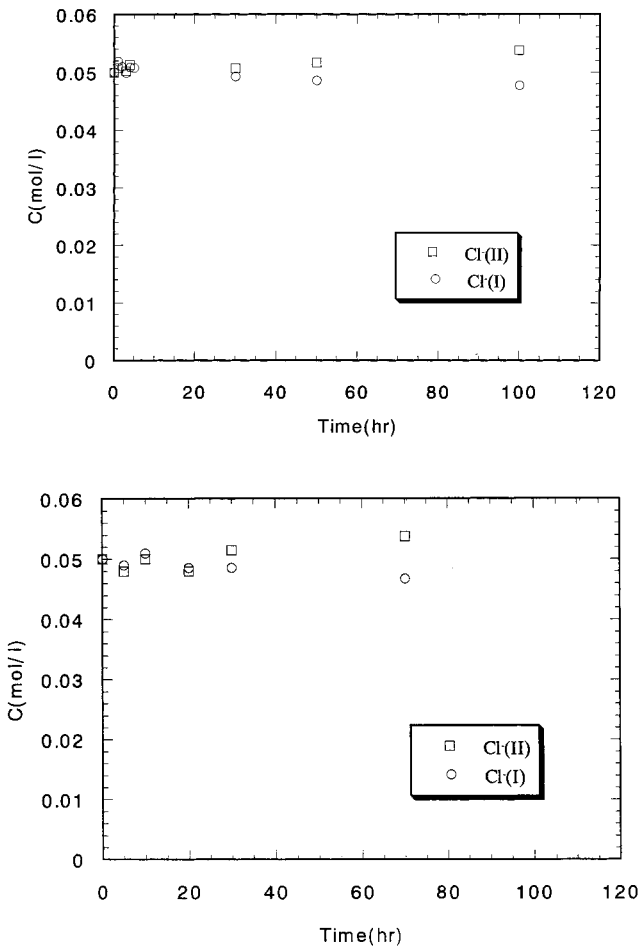

Figure 6. Changes in anion concentration on both sides (I and II) of the membranes as a function of time: (a, top) K-101 and (b, bottom) Nafion.

membrane potential for KCl to the following equation[22,24]

$$\Delta\phi = -\frac{RT}{F}\ln\left[\frac{C_d}{C_0}\frac{\sqrt{1+\left(\frac{2C_0}{QC_x}\right)^2}+1}{\sqrt{1+\left(\frac{2C_d}{QC_x}\right)^2}+1}\right] - \frac{RT}{F}W\ln\left[\frac{\sqrt{1+\left(\frac{2C_d}{QC_x}\right)^2}+W}{\sqrt{1+\left(\frac{2C_d}{QC_x}\right)^2}+W}\right] \quad (8)$$

where $W = (\omega_K - \omega_{Cl})(\omega_K + \omega_{Cl})$, C_d and C_0 are KCl concentrations on the low and high concentration sides, respectively, and Q is charge effectiveness. The mobility ratio of anion to cation, ω_-/ω_+, (=1.04), in the membrane is assumed to be the same as that in water. Measurements were carried out under the condition where C_0/C_d equals 2. Charge density, C_x, was determined by titration of a membrane as Saito carried out.[27,28] The membrane water content and degree of hydration were given by the same method that Saito used.[27,28] The thickness of the swollen membrane was obtained by the conductance of the membrane, which was measured by the AC method. Measurements were carried out with an impedance analyzer (4192A LF, Yokogawa Hewlett-Packard Co.) operating in a frequency range between 10 and 100 kHz. We used 0.5 M KCl and 0.5 M HCl as the external solution. As shown in Table 1, both the effective charge density and the charge density of K-101 were about twice as much as those of Nafion. Water content and degree of hydration of Nafion is larger than those of K-101. The charge effectiveness, Q, for K-101 is 0.12 and for Nafion 0.093. Usually it is considered $Q = 0.1-0.2$ from various experimental results.[29,30] According to Mafé et al., if the dielectric constant near the fixed charge group is low, ion pairing with K^+ or H^+ is formed to reduce the charge effectiveness.[31−33] As seen in Figure 1 those polymers are hydrophobic except the sulfonic group and form the fine pores for water storage. Even if enough water to migrate ions can exist in the membrane pore, the hydrophobic polymer chains, which have low dielectric constant, can locate near the fixed charge group at the membrane surface, since the polymer surface entropy is larger than that of the polymer inside.[34,35] Fluctuating the polymer chain around a fixed charge group reduces the dielectric constant in the vicinity. The ion pairing formed near the membrane surface affects on the Donnan potential, and the effective charge density, QC_x (mol/L), is estimated lower. The charge density, C_x (mol/L), is defined as the number of charge groups per unit volume of water in the membrane. The inverse charge density, $1/C_x$, corresponds to the water volume per one fixed charge group. $1/C_x$ for K-101 is 0.18 and for Nafion 0.32, which indicates that the water volume around the sulfonic group in Nafion is 1.8 times as large as that in K-101. Thickness was approximately equivalent between these two membranes. Ionic conductivity across a membrane is a function of (effective) fixed charge density, ionic concentration, and ionic mobility. In K-101, there was no difference in conductivity between in 0.5 M KCl and in 0.5 M HCl. HCl conductivity (180 mS/cm) is much larger than that of KCl (60 mS/cm) in water because of the large mobility of H^+ in water. H^+ mobility is also considered to be larger than that of K^+ in the membrane. If the both ionic concentrations in the membrane are the same as those in water, conductivities should be different. In this case KCl concentration in the membrane is supposed to be much larger than that of HCl in the K-101 membrane. In Nafion, however, the conductivity in 0.5 M HCl was 5.4 times as much as that in 0.5 M KCl. HCl conductivity is larger than that in the water, and KCl conductivity is smaller than that in the water. The high HCl conductivity in the Nafion is attributed to the high water hydration in the pore and specific proton transfer caused by ordered water structure,[4] and comparably the low KCl conductivity to the tortuous fine pore structure.

4.2. Comparison with Theoretical Predictions. To explain the experimental results mentioned above, we calculated the time evolution of ion concentrations using the TMS theory. The parameters in this experimental system are shown in Table 1, and the results of theoretical predictions are shown in Figures 7 and 8. Cation concentrations for K-101 are given as a function of time in Figure 7a and for Nafion in Figure 7b. The solid and broken lines represent H^+ and K^+ curves, respectively. Similarly, anion concentrations for K-101 are given as a function of time in Figure 8a and for Nafion in Figure 8b. The solid and broken lines represent the curve of Cl^- in side I and that in side II, respectively. Compared with the experimental results for cations (see Figure 4), we could see that our model roughly followed the experimental trends; that is, cation concentrations are going to converge to the constant value, and K^+ concentration change is slower than that of H^+ with time increase. However, we could not predict the experimental results exactly from our model though it was much better for K-101 than for Nafion. With regard to anions, we confirmed that a small

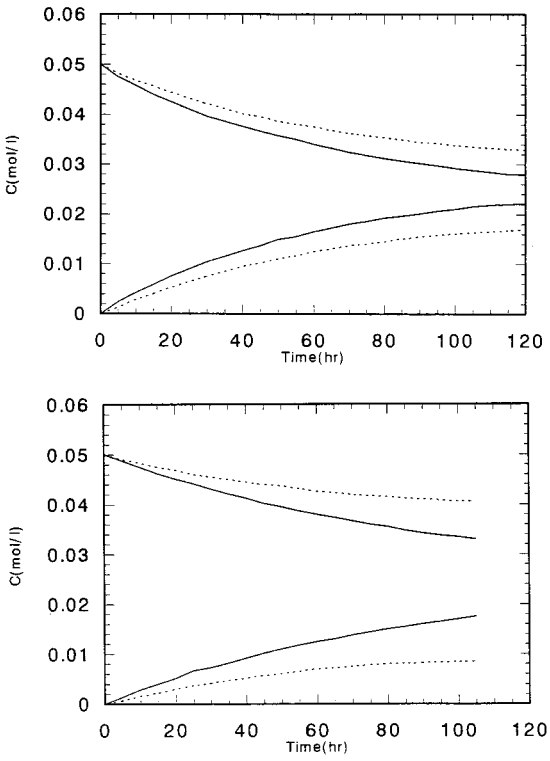

Figure 7. Theoretical prediction of cation concentration changes (H^+, solid line; K^+, broken line) on both sides (I and II) of the membranes as a function of time: (a, top) K-101 and (b, bottom) Nafion.

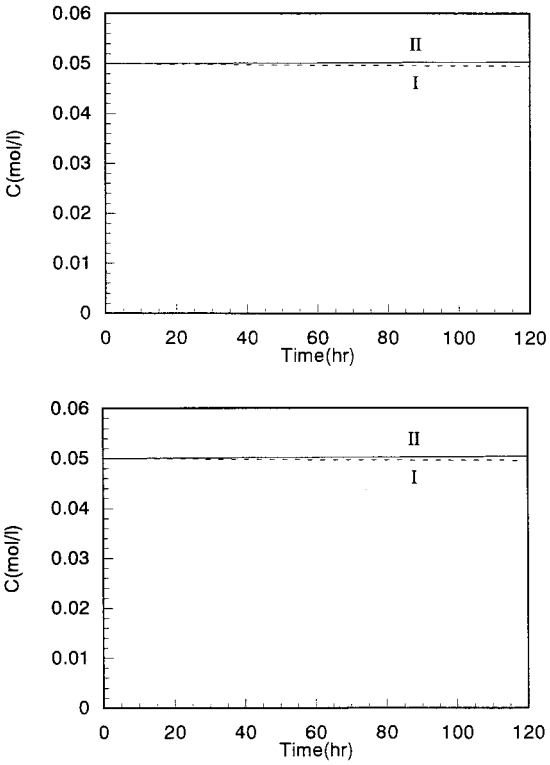

Figure 8. Theoretical prediction of anion concentration changes (H^+, solid line; K^+, broken line) on both sides (I and II) of the membranes as a function of time: (a, top) K-101 and (b, bottom) Nafion.

amount of Cl^- migrated across the cation exchange membrane in our model, too, though the theoretical results could not correspond to the experimental results exactly. We also computed the changes in K^+ and H^+ concentrations using effective charge density as a parameter. Figure 9a,b exhibits

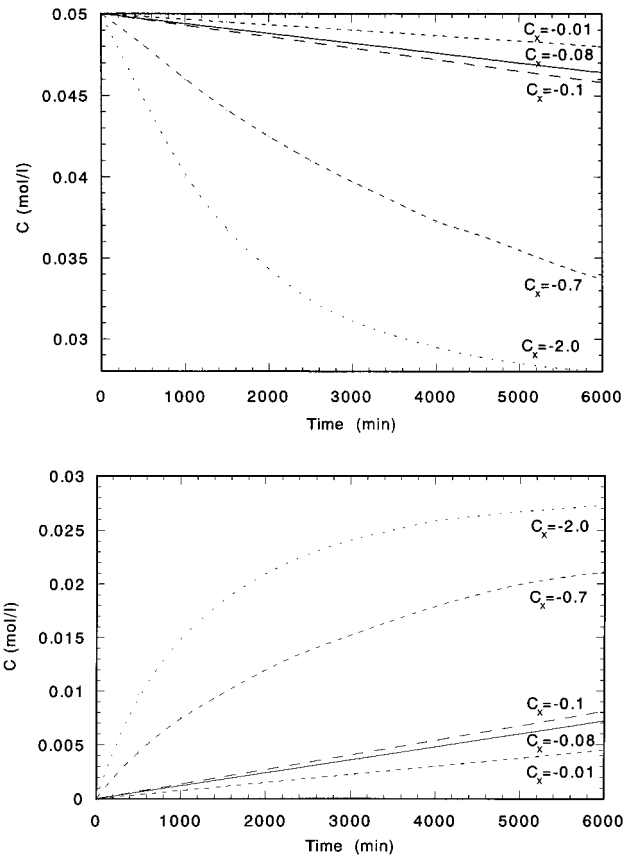

Figure 9. (a, top) K^+ and (b, bottom) H^+ concentration changes at side II as a function of time for various charge densities ($C_x = -0.01$, -0.08, -0.1, -0.7, and -2.0), where the initial concentration is 0.05 mol/L for both ions.

the results that K^+ and H^+ concentrations change rapidly with increase of effective charge density. Evidently ion flux increases with increase of effective charge density. This contradicted the fact that the ion flux in Nafion, whose effective charge density is smaller than that of K-101 (see Table 1), is larger than that in K-101. One of the roots of this inconsistency could be found in the assumption used in determining the effective charge density. One could assume that fixed charge groups were distributed homogeneously in the ideal charged membrane. The effective charge density given here could not reflect the effects of the distribution of charge groups or the morphology of the hydrophilic part of the charged membrane. Consequently, we have to take this effect into account to develop the TMS theory. Incidentally, we could consider that the cause of the other disagreement could be found in the following assumption: the mobility ratio of anion to cation, ω_-/ω_+, in the membrane is the same as that in water. In a practical case, the two must be different in the membrane. As shown in Table 1 the conductivity of Nafion with HCl aqueous solution is higher than that of HCl aqueous solution. It suggests that there exists a special proton transport mechanism in the membrane pore; that is, the water molecules remain at the fixed position but only the electric charge is migrated through water network in the pore.[4] During the charge migration K^+ is dragged to the opposite side in order to maintain the electroneutrality. Thus K^+ transport is accelerated. If the proton transport is occurred by such charge migration through the structured water phase in the membrane pore, it is a countertransport of cation and charge. In the case of K-101, water molecules cannot be supplied sufficiently in the ion channel so that such effect for transport has to be reduced. However, it is necessary to determine the ionic

mobility in the membranes for a better description of transport phenomena through the charged membrane.

Acknowledgment. Special thanks go to Mr. M. Hamada and Mr. K. Yoshie at Asahi Chemicals Co. for providing us with the samples and for helpful suggestions.

References and Notes

(1) Stryer, L. *Biochemistry*, 3rd ed.; W. H. Freeman and Company: New York, 1988.
(2) Minagawa, M.; Tanioka, A.; Ramírez, P.; Mafé, S. J. *Colloid Interface Sci*. **1997**, *188*, 176.
(3) Robinson, R. A.; Stokes, R. H. *Electrolyte Solutions*, 2nd ed.; Butterworths: London 1959.
(4) Barrow, G. M. *Physical Chemistry*, 5th ed.; McGraw-Hill: New York, 1988; Chapter 9.7.
(5) Gennis, R. B. *Biomembranes: Molecular Structure and Function*; Springer-Verlag, New York, 1989.
(6) Grot, W. *Chem.-Ing. Tech.* **1978**, *50*, 299.
(7) LaConti, A. B.; Fragala, A. R.; Boyack, J. R. *Proc. Electrochem. Soc*. **1977**, *77*, 354.
(8) Will, F. G. *J. Electrochem. Soc*. **1979**, *126*, 35.
(9) Yeo, R. S.; Chin, D.-T. *J. Electrochem. Soc*. **1980**, *127*, 549.
(10) Yeo, R. S.; McBreen, J.; Kissel, G.; Kulesa, F.; Srinivasan, S. *J. Appl. Electrochem*. **1980**, *10*, 741.
(11) Eriksen, O. I.; Aksens, E.; Dahl, I. M. *J. Membrane Sci*. **1993**, *85*, 89.
(12) Eriksen, O. I.; Aksens, E.; Dahl, I. M. *J. Membrane Sci*. **1993**, *85*, 99.
(13) Gierke, T. G.; Munn, G. E.; Wilson, F. C. *J. Polym. Sci.: Polym. Phys. Ed*. **1981**, *19*, 1687.
(14) Donann, F. C. *Z. Electrochem*. **1911**, *17*, 572.
(15) Donann, F. C. *Z. Phys. Chem.* **1934**, *A168*, 369.
(16) Reiss, H.; Bassignana, I. C. *J. Membrane Sci*. **1982**, *11*, 219.
(17) Mauritz, K. A.; Fu, R.-M. *Macromolecules* **1988**, *21*, 1324.
(18) Mauritz, K. A.; Yun, H. *Macromolecules* **1988**, *21*, 2738.
(19) Zawodziski, T. A.; Neeman, M., Jr.; Sillerud, L. O.; Gottesfeld, S. J. *Phys. Chem.* **1991**, *95*, 6040.
(20) Zawodziski, T. A., Jr.; Derouin, C.; Radizinski, S.; Sherman, R. J.; Smith, V. T.; Springer, T. E.; Gottesfeld, S. *J. Electrochem. Soc*. **1993**, *140*, 1041.
(21) Chen, R. S.; Jayacody, J. P.; Greenbaum, S. G.; Pak, Y. S.; Xu, G.; McLin, M. G.; Fontanella, J. J. *J. Electrochem. Soc*. **1993**, *140*, 889.
(22) Teorell, T. *Proc. Soc. Biol*. **1935**, *33*, 282.
(23) Teorell, T. *Prog. Biophys. Biophys. Chem.* **1953**, *3*, 305.
(24) Meyer, K. H.; Sievers, J. F. *Helv. Chim. Acta* **1936**, *19*, 649, 665, 987.
(25) Demisch, H.-U.; Pusch, W. *J. Electrochem. Soc*. **1976**, *123*, 370.
(26) Nernst, H. W. *Z. Phys. Chem*. **1889**, *2*, 2; *154*, 4.
(27) Saito, K.; Tanioka, A.; Miyasaka, K. *Polymer* **1994**, *35*, 5098.
(28) Kawaguchi, M.; Murata, T.; Tanioka, A. *J. Chem. Soc., Faraday Trans*. **1997**, *93*, 1351.
(29) Yuasa, M.; Kobatake, Y.; Fujita, H. *J. Phys. Chem*. **1968**, *72*, 2871.
(30) Ueda, T.; Kamo, N.; Ishida, N.; Kobatake, Y. *J. Phys. Chem*. **1972**, *76*, 2447.
(31) Mafé, S.; Ramírez, P.; Tanioka, A.; Pellicer, J. *J. Phys. Chem. B* **1997**, *101*, 1851.
(32) Chou, T.-J.; Tanioka, A. *J. Phys. Chem. B* **1998**, *102*, 129.
(33) Jimbo, T.; Higa, M.; Minoura, N.; Tanioka, A. *Macromolecules* **1998**, *31*, 1277.
(34) Garbassi, F.; Morra, M.; Occhiello, E. *Polymer Surfaces—From Physics to Technology*; John Wiley & Sons: Chishester, 1994.
(35) Meyers, G. F.; DeKoven, B. M.; Seitz, J. T. *Langmuir* **1992**, *8*, 2330.